Fermi National Accelerator Laboratory

FERMILAB-Conf-00/065

Neutrino Radiation at Muon Colliders and Storage Rings

Nikolai Mokhov and Andreas Van Ginneken

Fermi National Accelerator Laboratory
P.O. Box 500, Batavia, Illinois 60510

April 2000

Presented at and to Appear in the Published Proceedings of *ICRS-9 International Conference on Radiation Shielding*, Tsukuba, Ibaraki, Japan, October 17-22, 1999

Operated by Universities Research Association Inc. under Contract No. DE-AC02-76CH03000 with the United States Department of Energy

Neutrino Radiation at Muon Colliders and Storage Rings

Nikolai MOKHOV* and Andreas VAN GINNEKEN

Fermi National Accelerator Laboratory

Abstract

Intense highly collimated neutrino beams, created from muon decays at high-energy muon colliders or storage rings, cause significant radiation problems even at very large distances from the machine. A recently developed weighted neutrino interaction generator permits detailed Monte Carlo simulations of the interactions of neutrinos and of their progeny with the MARS code. Special aspects of neutrino radiation dose evaluation are discussed. Dose distributions in a tissue-equivalent phantom are calculated when irradiated with 100 MeV to 10 TeV neutrino beams. Results are obtained for a bare phantom, one embedded in several shielding materials, and one located at various distances behind a shield. Neutrino radiation is investigated around muon storage rings serving as the basis for neutrino factories. The most challenging problem of off-site neutrino dose from muon colliders and storage rings is studied. The distance from the collider ring (up to 60 km) at which the expected dose rates equals prescribed annual dose limits is calculated for 0.5-4 TeV muon colliders and 30 and 50 GeV muon storage rings. Possible mitigation of neutrino radiation problems are discussed and investigated.

1 INTRODUCTION

Neutrinos from muon decay may cause—to the surprise of many—significant radiation problems even at large distances from a muon collider or muon storage ring (MuSR) [1, 2]. Dose at a given location grows with muon energy roughly as E^3 due to (1) the increase with energy of the neutrino cross section, (2) total energy deposited, and (3) the collimation of the decay neutrinos—each responsible for a factor of E. The more energetic decay neutrinos emanate radially outward from the collider ring at angles with respect to the μ direction of order m_μ/E. Extremely low interaction and scattering probabilities mean that neutrinos travel essentially in a straight line and survive over enormous distances. One consequence of this is that neutrino radiation safety is almost exclusively concerned with predicting and minimizing beam-on *off-site dose*. On-site dose has a higher regulatory threshold and can be dealt with in the usual ways of posted warnings, fences, interlocks, etc. Other problem classes, such as radioactivation of ground water, occur at too low levels to be a concern and if direct off-site ν-radiation is everywhere under control, the same can be assured for the other types of problems. From simple geometry, dose is expected to decline with inverse square of radial distance and for a 2+2 TeV collider the (Fermilab off-site) annual dose limit of 0.1 mSv (10 mrem) is reached only after 34 km [3] to 57 km [4]. It becomes clear that ν-radiation will impact strongly on siting issues and cost of a high energy muon collider and therefore needs to be taken very seriously. It is the purpose of this paper to briefly describe the algorithms produced to perform Monte Carlo calculations of neutrino radiation then, putting the algorithms to work, present some results for rather idealized situations. The main goal of the latter is to answer some 'frequently asked questions' as well as to provide a basis from which to make estimates about neutrino radiation for more specific scenarios. A discussion of radiation safety cannot avoid entirely its regulatory aspects which are bound to play a crucial role in devising strategies to deal with the problem. These matters are highly site specific: regulations depend on the country where the device is to be located and off-site radiation levels will be influenced by size, shape, location, etc., of the site as well as its geology and that of its surroundings.

Care must be taken in evaluating long-term averaged neutrino dose. Neutrinos from decay of high energy muons spread very little with distance traversed and at the site boundary the height of the 'disk' may be much less than typical human dimensions. As a result, there may be considerable difference between maximum and averaged 'whole-body' dose in a human and how the latter is calculated. This is in contrast to off-site dose at present-day facilities where hadrons, $e^\pm$, γ, or $\mu^\pm$ conveying the dose are spread over an area well exceeding human dimensions. Therefore specification of neutrino dose may well require that regulatory interpretation be sharpened as to how long term exposures must be evaluated. The 'equilibrium assumption' of Ref. [1] is equivalent to assessing the dose in some small volume of human tissue embedded in an essentially infinite medium of tissue and irradiated by a broad beam of neutrinos. By contrast Ref. [5] assumes a phantom surrounded by vacuum. These rather sweeping assumptions bear greatly on dose within the phantom. In a more realistic situation one must specify the neutrino beam phase space while the phantom may be embedded in, e.g., soil, concrete, steel, lead—or placed in an evacuated region (or in air) perhaps with some specified thickness of material interposed. The

* *Corresponding author, MS 220, P.O. Box 500, Batavia, IL 60510, USA, Tel. (630) 840-4409, Fax. (630) 840-6039, E-mail: mokhov@fnal.gov*

latter scenario may apply, e.g., when neutrinos emerge from an underground ring, travel some distance through the air, then come upon a tall building and its occupants. Each of these geometries affects neutrino interaction probabilities and subsequent shower development in different ways which in turn affect evaluation of both maximum and averaged dose.

It is clear that—like in all other shielding calculations—a thorough investigation of the problem must rely on detailed Monte Carlo simulations of the neutrino interactions and their progeny. To this end a (weighted) neutrino interaction generator is developed and incorporated in the MARS [6] code. This is briefly described in Sec. II. Inclusion into MARS ensures that (a) interactions and transport of hadrons, electrons, photons, and muons produced by the neutrinos are readily taken care of by MARS using algorithms which are all well benchmarked and (b) neutrino 'shielding' calculations can be pursued using all the tools and techniques already present in the code. Sec. III discusses special aspects of neutrino radiation and dose evaluation. Sec. IV presents results for various geometries with mono-energetic neutrino beams. In Sec. V problems associated with a straight muon beam are addressed along with those related to MuSR which are contemplated as a source of neutrinos, mostly to serve distant detectors. Such a storage ring is therefore equipped with a long straight section aligned with a detector within which one aims to maximize the number of neutrino interactions. Mitigation of possibly high off-site dose rates due to storage rings are discussed in this section. What to expect around colliders is the subject of Sec. VI. Here muon energy, physical layout of the ring, and beam optics strongly affect spatial, angular, and energy distribution of the neutrinos and thus bear on dose rates at distant locations around the ring. Mitigations of off-site dose around colliders are discussed and illustrated. Concluding comments are in Sec. VII.

2 NEUTRINO INTERACTION MODEL

The neutrino interaction model serves to represent energy and angle of the particles—$\nu, e^{\pm}, \mu^{\pm}$, and hadrons—emanating from a simulated interaction. These particles, along with the showers initiated by them, are then further processed by the MARS code which calculates, e.g., energy deposition and dose as a function of location in a user specified geometry. Four types of neutrinos are included and distinguished throughout: $\nu_\mu, \overline{\nu}_\mu, \nu_e, \overline{\nu}_e$, which are represented in the decays from a $\mu^+\mu^-$ collider in roughly equal amounts. The model identifies *eight* types of interactions as listed in Table 1 for $\nu_\mu, \overline{\nu}_\mu$. There is an entirely similar array for $\nu_e, \overline{\nu}_e$.

The first row in Table 1 corresponds to charged current deep inelastic neutrino interactions. 'X' represents a final hadronic state which includes particles produced in the interaction (π, K, ...) as well as nucleons knocked out of the target nucleus. Total cross sections σ are assumed to be $6.7 \cdot 10^{-39} E_\nu$ per nucleon for ν and $3.4 \cdot 10^{-39} E_{\overline{\nu}}$ for $\overline{\nu}$ with the E in GeV [7] and the σ in cm^2. These are close to Refs. [1, 5]. The differential cross section is taken from [8, 9]

Table 1: *Neutrino Interactions*

$\nu_\mu N$	$\rightarrow$	$\mu^+ X$	$\overline{\nu}_\mu N$	$\rightarrow$	$\mu^- X$
$\nu_\mu N$	$\rightarrow$	$\nu_\mu X$	$\overline{\nu}_\mu N$	$\rightarrow$	$\overline{\nu}_\mu X$
$\nu_\mu p$	$\rightarrow$	$\mu^+ n$	$\overline{\nu}_\mu n$	$\rightarrow$	$\mu^- p$
$\nu_\mu p$	$\rightarrow$	$\nu_\mu p$	$\overline{\nu}_\mu p$	$\rightarrow$	$\overline{\nu}_\mu p$
$\nu_\mu n$	$\rightarrow$	$\nu_\mu n$	$\overline{\nu}_\mu n$	$\rightarrow$	$\overline{\nu}_\mu n$
$\nu_\mu e^-$	$\rightarrow$	$\nu_\mu e^-$	$\overline{\nu}_\mu e^-$	$\rightarrow$	$\overline{\nu}_\mu e^-$
$\nu_\mu e^-$	$\rightarrow$	$\nu_e \mu^-$			
$\nu_\mu A$	$\rightarrow$	$\nu_\mu A$	$\overline{\nu}_\mu A$	$\rightarrow$	$\overline{\nu}_\mu A$

$$\frac{d\sigma}{dx\,dy} = \frac{G^2 x s}{2\pi}\left(Q(x) + (1-y)^2\,\overline{Q}(x)\right) \qquad (1)$$

where $x = -q^2/2M\nu$ with q the momentum transfer, M the nucleon mass, and ν the energy loss of the neutrino in the lab, $y = \nu/E_\nu$, G is the Fermi coupling constant, s is the total energy in the center of mass, and $Q(x), \overline{Q}(x)$ represent quark, anti-quark momentum distributions inside the nucleon. Both $xQ(x)$ and $x\overline{Q}(x)$ are taken from experiment in numerical form. For anti-neutrinos the roles of $Q(x), \overline{Q}(x)$ in Eq. 1 are interchanged. Once the direction and momentum of the lepton is decided in the Monte Carlo, total (vectorial) momentum of the interaction is balanced by a single π which is then forced to undergo (via MARS) a deep inelastic interaction in the same target nucleus. The particles produced by this π are then permitted to shower, etc., as they traverse the material. Since interest here is confined to certain gross averages over the showers (energy deposition, dose equivalent, etc.) this rather coarse way of dealing with the 'hadronization' appears justifiable.

The second row in Table 1 contains the neutral current deep inelastic interactions. Total cross sections are taken as $2.2{\cdot}10^{-39} E_\nu$ and $1.35{\cdot}10^{-39} E_{\overline{\nu}}$ for ν and $\overline{\nu}$, respectively—again in units of cm^2 with E in GeV and again close to [1, 5]. The differential cross sections

$$\frac{d\sigma}{dx\,dy} = \frac{G^2 x s}{2\pi} g_L^2 \left(Q(x) + (1-y)^2 \overline{Q}(x)\right) + \frac{G^2 x s}{2\pi} g_R^2 \left(\overline{Q}(x) + (1-y)^2 Q(x)\right) \qquad (2)$$

with $g_L^2 = 0.30$ and $g_R^2 = 0.024$ and where $Q(x)$ and $\overline{Q}(x)$ are again to be interchanged for antineutrinos. Hadronization is as for the charged current interactions. These first two items form the main contributions to the dose from neutrino interactions.

The next three on the list correspond to neutrino-nucleon elastic and quasi-elastic scattering. The differential cross section is [10]

$$\frac{d\sigma}{d|q^2|} = \frac{G^2 x M^2}{8\pi E_\nu^2}\left(A \pm B\frac{s-u}{M^2} + C\frac{(s-u)^2}{M^4}\right) \qquad (3)$$

The $+$ in $\pm$ refers to ν and $-$ to $\overline{\nu}$, while A, B, C are functions of various q^2-dependent form factors which are taken as per Ref. [11]. Total cross sections are obtained by integrating Eq. 3. Because Eq. 3 is difficult to sample directly, results from it are fitted to simple analytical forms. For nuclear targets a 'Pauli factor' is included (as a weight) to discourage small $|q^2|$ which are insufficient to liberate a nucleon or promote the nucleus to an excited state [12].

The next two items in Table 1, neutrino interactions with atomic electrons, contribute little to total dose but are included for completeness. Cross sections for the neutral current process can be summarized in the form [13]:

$$\frac{d\sigma}{dy} = \frac{G^2 m_e E_\nu}{8\pi}\left(a + b\,(1-y)^2\right) \tag{4}$$

where a, b are simple combinations of coupling constants. For ν_μ and $\overline{\nu}_\mu$, $a \simeq b \simeq 1$ while for ν_e, $a \simeq 9$, $b \simeq 1$ with a and b reversed for $\overline{\nu}_e$. For the charged current, only $\nu_\mu e^- \rightarrow \nu_e \mu^-$ and $\overline{\nu}_e e^- \rightarrow \overline{\nu}_\mu \mu^-$ need be considered. The cross sections are [14]:

$$\frac{d\sigma}{dy} = 2\frac{G^2 m_e E_\nu}{\pi} \tag{5}$$

for ν_μ and

$$\frac{d\sigma}{dy} = 2\frac{G^2 m_e E_\nu}{\pi}\,(1-y)^2 \tag{6}$$

for $\overline{\nu}_e$.

Finally, coherent elastic scattering—last item in the Table—is included in the manner of [15]

$$\frac{d\sigma}{d\Delta^2} = \frac{G^2 N^2}{8\pi}\left(1 - \frac{\Delta^2}{\Delta^2_{max}}\right) \tag{7}$$

where N is the number of neutrons in the nucleus and Δ is the momentum transfer to the nucleus with $\Delta_{max} = R_A^{-1}$, the inverse nuclear radius. For all 'elastic' interactions only the recoil is of interest and is readily simulated.

Perhaps the above should also include inelastic neutrino interactions which produce—one or a few—pions via resonances since these are not well represented by the deep inelastic prescription and since these can also proceed coherently off a nucleus [16]. However, both total cross section and energy deposition resulting from such processes are relatively small compared with the deep inelastic interactions.

3 NEUTRINO DOSE

Much like neutrons and gammas, neutrinos by themselves cause little or no biological damage but instead create charged particles which in turn deposit their energy in tissue to be interpreted as dose 'due to neutrinos'. When studying radiation dose delivered to a person in a broad-beam geometry, the person to whom it is delivered is usually represented by a 30 cm thick tissue-equivalent phantom (TEP). While removal of neutrinos by absorption or spreading by scattering are entirely negligible over distances considered here, one must not neglect any material present immediately upstream of the phantom where neutrinos might interact and initiate both hadronic and electromagnetic showers. A broad, parallel beam of neutrinos (in the GeV region and above) striking a target thus causes a buildup of dose at relatively shallow depths eventually to reach a plateau after which dose is expected to remain constant, i.e., an equilibrium is achieved.

Equilibrium may be defined as the condition whereby dose is approximately proportional to ν-fluence in the general vicinity of maximum fluence. Thus in the general case the equilibrium dose is *not* constant with depth but changes at the same rate as ν-fluence. The distance required to establish equilibrium is essentially one full length of the cascade peak, i.e., the distance to where energy deposition density has fallen to a small fraction of its maximum value when ν's are forced to interact at zero depth. For practical purposes, high energy muons created in $\nu_\mu, \overline{\nu}_\mu$ interactions do not participate in establishing this equilibrium since they travel for large distances and their contribution to dose lies, for the most part, well outside typical transverse dimensions of the ν-beam and its other progeny. Interesting questions concern the equilibrium dose for various materials—especially those commonly encountered—and the thickness needed to reach it, as a function of neutrino energy.

The computational advantages of the equilibrium assumption are obvious. Instead of relying on Monte Carlo simulations of neutrino generated cascades, one can estimate [1] an equilibrium dose assuming that—upon interaction—all of the neutrino energy (minus some fraction carried off by outgoing ν's) is deposited locally. It may be converted to dose by applying some quality factor which properly averages over the particles which participate in neutrino induced cascades. This would be a good approximation if the material immediately upstream (for some ten interaction lengths or more at high energy) were tissue-equivalent and if the neutrino 'beam' were of human dimensions or larger. Similarly (and reminiscent of the so-called Bragg-Gray Principle) one may assume the ν's to interact in *soil* and again apply an effective quality factor (different from the one for tissue, above) to convert energy deposited in soil to dose equivalent. Since—in a typical scenario—soil (or concrete, which is nearly equivalent) is the most likely material present upstream this may be an acceptable approximation for broad beam ν's.

In regulatory contexts one recognizes both *maximum* dose delivered to some small volume in the body—perhaps a sensitive organ—and *whole-body* dose which is averaged over the entire body [17]. The former is concerned mostly with accidental irradiation and the latter with long-term exposure. For off-site dose around proton or electron machines the two are closely related since particles delivering the dose at and beyond the site boundary are almost always spread out over a region larger than human dimensions thus effectively equating average and maximum dose. Additionally, off-site dose is measured over rather long duration and

limits are usually expressed in terms of an *annual* dose. For a ν's from a muon collider or storage ring the *spatial* averaging cannot be taken for granted since the more energetic ν's remain strongly collimated over many kilometers. However, over the course of a year minimal levels of human activity will perform the averaging equally well. Therefore whole-body dose—spatially averaged in some way and calculated at off-site locations—remains a practical and conservative upper limit.

To calculate maximum dose, whether in a bare TEP or one situated in a complex geometry, one needs to specify only the phantom's thickness (30 cm). To calculate whole-body dose—in the 'narrow beam' case—the two other dimensions of the phantom must be stipulated as well. One choice, used in neutron dosimetry, is a cylindrical phantom of 30 cm diameter and 60 cm height [18]. For this work a block-shaped phantom of thickness=width=30 cm and height=60 cm is used. The main advantage is that—once axial symmetry is lost—this 'squared off' version divides more readily into volume bins which take advantage of the other symmetries exhibited in the more interesting beam-phantom geometries. This facilitates calculating maximum and whole-body dose simultaneously. It also corresponds better to the 30 cm thick, transversely infinite, phantom used in the broad beam limit. When simulating a real situation the ν-beams would be spread-out due to decay angles and divergence of the muon beam—though typically insufficient to approximate a beam which uniformly covers the phantom. However, both pencil beams and planar beams may serve as worst-case-scenarios since centrally incident beams on a phantom (embedded or not) will necessarily produce a higher maximum and whole-body dose than spread-out beams. This will provide an interesting comparison with equilibrium dose under the same circumstances. Note that, for a disk-like beam whole-body dose depends on orientation. For example, the phantom intercepts twice as many ν's in a prone (disk intercepts mid-phantom along the 60-cm dimension) *vs* seated position (disk cuts along the 30-cm dimension). In a bare phantom this might result in about twice the whole-body dose (not exactly because leakage of ν-generated cascades depends on orientation). For embedded phantoms, a somewhat larger fraction of the cascades initiated upstream enters the phantom when in seated position. An interesting and easy-to-define case is where the ν-beam—more precisely the center of the beam—is swept evenly across the phantom to simulate (still conservatively) *time* averaging.

4 NEUTRINO BEAMS

Although monoenergetic neutrino beams as such have no practical bearing on radiation problems connected with any contemplated facilities, it is a good starting place to gain some insight into these problems. Fig. 1 shows a whole-body dose equivalent as a function of energy for a ν_μ *broad* beams incident on a bare seated TEP, i.e., one suspended in vacuum (non-equilibrium case). The whole-body dose is about a factor of two lower than the maximum dose calculated in [4, 5] under the same conditions.

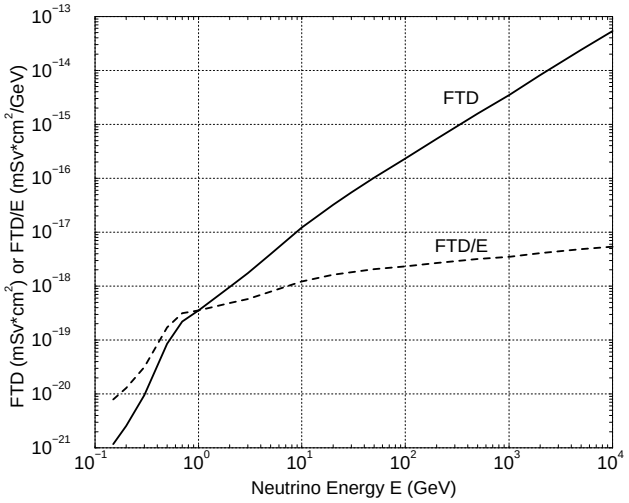

Figure 1: Whole-body dose equivalent in a bare seated TEP per unit ν_μ-fluence, or flux-to-dose (FTD) value. Dashed curve is FTD/E.

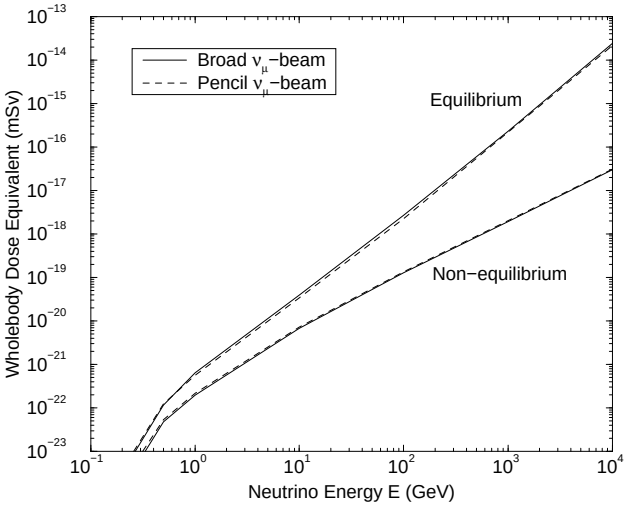

Figure 2: Total whole-body dose in a bare seated TEP (non-equilibrium) and in one embedded in infinite soil (equilibrium) *vs* neutrino energy for broad (solid) and pencil (dashed) ν_μ-beams.

Calculations show that the equilibrium dose is practically achieved after some 3-4 m of soil at all energies of interest here. Such a wall is thus equivalent to all walls of equal or greater thickness and may hence be referred to as a 'thick' wall. Fig. 2 presents a whole-body dose equivalent versus ν_μ-energy for *broad* and *pencil* beams incident on a bare TEP in seated (or prone, which is equivalent here) position as well as on a TEP in equilibrium with the surrounding soil. Instead of providing shielding, the presence of soil upstream enhances the dose by a factor of $\sim$1000 in the TeV region as compared to the bare TEP. One sees that there is

practically no difference between broad and pencil beams in this case.

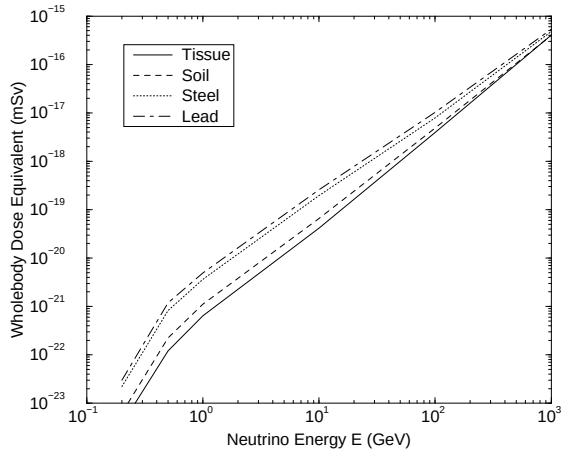

Figure 3: Whole-body dose in an axial TEP embedded in infinite materials *vs* neutrino energy for a broad ν_μ-beam.

The E^2-behavior, strictly observed by the equilibrium dose, is also followed closely by the MARS results. Deviations are most likely due to more detailed evaluation of the quality factor in MARS—versus a constant factor of *two* in [5]. The energy dependence of the difference supports this: at low energy a larger fraction of the dose is delivered by (high quality factor) low energy neutrons whereas at high energy the electromagnetic component (with quality factor essentially unity) dominates.

Fig. 3 shows whole-body dose equivalent in a TEP located immediately downstream of a thick wall of various compositions for a broad ν_μ beam parallel to the long (60 cm) axis of the phantom (*axial* geometry). One sees that the dose after thick medium and high-Z shielding is up to a factor of ten higher than that for a low-Z shielding at low neutrino energies, while the values converge in the TeV energy range.

5 MUON STORAGE RINGS (MUSR)

While dose due to mono-energetic neutrino beams yields important information—such as fluence-to-dose conversion factors—for further calculation it is neutrinos from muon beams which are of more practical interest. Intense muon beams and neutrino beams might be available for fixed target experiments as part of a collider complex and appear as an unavoidable part of collider operations each time the muons remaining at the end of a store are dumped. Muon storage rings—which create very similar radiation problems—are expressly conceived to create a neutrino beam pointing at some distant detector mostly to study ν-oscillation phenomena. All such scenarios start from a (nearly) mono-energetic muon beam. If the muon beam is directed to a dump, decay may occur while still in an evacuated region or while the beam slows down in the dump and spreads due to multiple scattering and other processes. Such a dump must be designed and situated also with *muon* radiation hazards in mind [20]. If no further use is made of the (muon or neutrino) beam, the muons may be magnetically defocused and/or guided along (even slightly) different directions over the course of a year to ensure that annual off-site ν-dose rates remain below the limit at all locations.

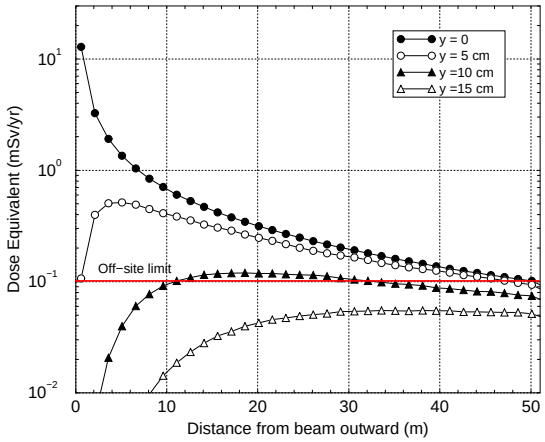

Figure 4: Annual maximum dose equivalent in a TEP embedded in soil outward from a 50 GeV MuSR arc tunnel at several heights with respect to the orbit plane.

A MuSR for ν experiments poses a ν radiation problem associated with its 'return leg'. The design which seems conceptually the simplest is that of a 'racetrack' in which the ring is coplanar but tilted with respect to the horizontal at such an angle that the straight section in which the μ's move downward aims at the faraway detector. The problem then is that muons traversing the other straight create a ν-beam which points out of the earth. While this beam may offer some interesting physics opportunities it also may present a radiation hazard. The beam will presumably emerge from the surface *on-site* so that access to this 'hot spot' can be controlled in the usual manner. Because of the tilt angle the beam, and its retinue of particles, then travels through the air to the site boundary where access can no longer be controlled and dose rate must conform to lower limits.

Realistic Monte Carlo simulations have been performed with the MARS code for the arcs and straight sections of a MuSR using the full lattice for 30 and 50 GeV muon beams. Forced muon decays and shower simulation is done in the arc FODO cells 9.8 m each consisting of 45 T/m 1-m quadrupoles and 6 T 2.4-m dipoles. At 50 GeV, muon decay rate is 1.6×10^{10} decays/(m·s. Results show that for *non-neutrino* radiation, the normal occupancy limit of 2.5μSv/hr is met by providing by 2 meters of dolomite type shielding below, above and radially inward from the arc tunnel enclosure walls. Six meters of such shielding is needed to meet

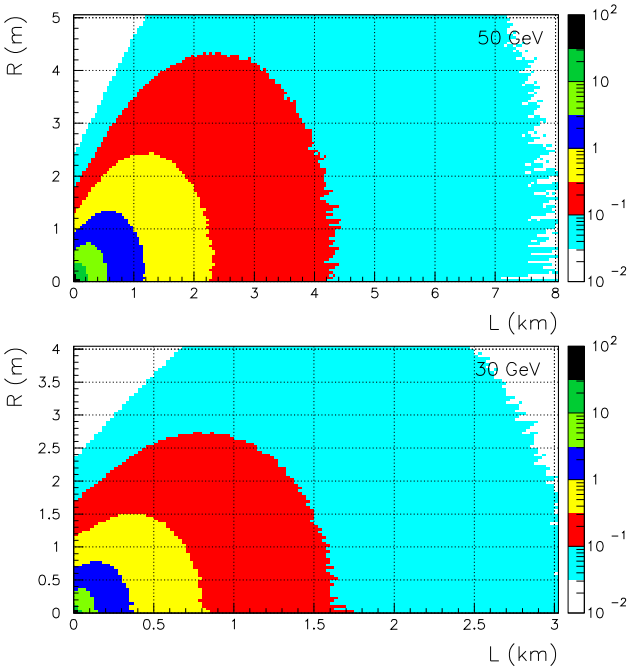

Figure 5: Isocontours of annual maximum dose equivalent in a TEP embedded in soil downstream of 30 and 50 GeV MuSR straight sections.

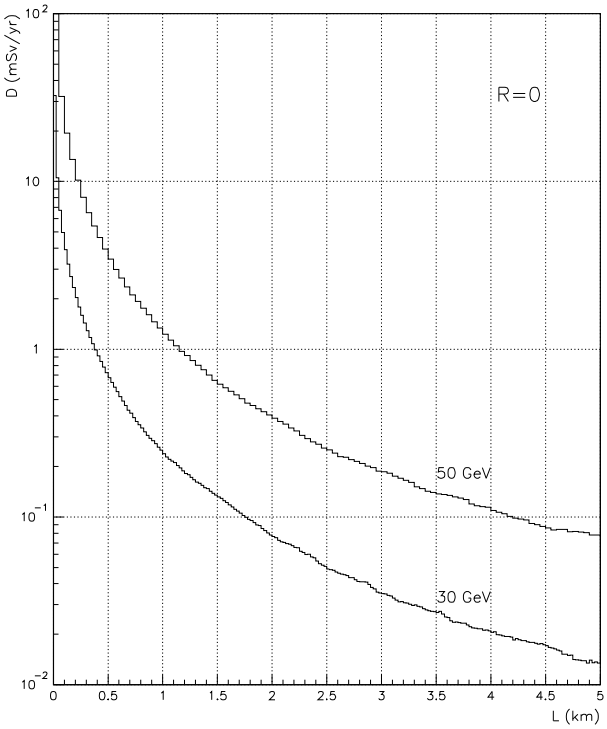

Figure 6: Axial distribution of annual maximum dose equivalent in a TEP embedded in soil downstream of 30 and 50 GeV MuSR straight sections.

that limit in the radially outward direction. Power supply rooms and other underground enclosures should be placed inward from the arc tunnel. The off-site limit of 0.1 mSv/yr due to *neutrino-induced* radiation in the arcs is reached at 50 meters radially outward from the beam orbit (Fig. 4). The half-height of the neutrino disk is only $\pm$10 cm from the orbit plane.

Isodose contours downstream of a 600-m long straight section with 2×10^{20} decays/yr at 30 and 50 GeV MuSR are shown in Fig. 5, while Fig. 6 shows the axial dose behavior. The off-site limit of 0.1 mSv/yr is met at 4.2 km for a 50 GeV MuSR and at 1.8 km for a 30 GeV MuSR. The maximum half-width of a 0.1 mSv/yr isocontour is 4.3 m and 2.7 m at 50 and 30 GeV, respectively.

Besides the racetrack there are at present several conceptions afloat including storage rings with multiple downward straight sections each pointing at a different detector (perhaps continents apart) after which, inevitably, the μ's must recirculate upward. Ref. [19] suggest that the ν's from the return straight be made to travel through a kilometer long evacuated pipe prior to crossing the surface so as to reduce dose due to muons and hadrons produced in soil. This suggestion needs to be examined carefully—preferably with a specific design and siting proposal in mind. Such a pipe might also act as a conduit for hadrons and muons which might be produced in the walls by ν's from decay of μ's at the edges of phase space and from the entire beam in the arc just prior to entering the straight. Other possible mitigations include a long upward arc (instead of straight section) so that the neutrinos emerge over a long swath where the arc-plane intersects the earth's surface. This dilution significantly reduces dose rates but may pose difficulties of an accelerator physics nature as well as significantly increased costs. Situating the arc so that ν's produced in it do not emerge off-site in large concentrations may likewise be non-trivial. This reservation extends to the regular arcs, e.g., in a racetrack design. Another mitigation is to introduce beam wobbling in either return straight section or arcs.

6 MUON COLLIDERS

The most daunting ν-radiation hazard is associated with high energy muon colliders. Given a model of the muon orbits the new ν-interaction generator in MARS readily provides realistic estimates of ν-induced dose around a muon collider. In a strictly planar μ-orbit, ν's spread exclusively due to transverse momentum acquired at decay with opening angle of roughly $1/\gamma_\mu$ which makes this a convenient 'worst case'. Neutrinos from decay of counter-rotating μ's strike the phantom at an angle of $2\sin^{-1}(R/L)$ between each other's directions (R is the ring radius, L is the distance from phantom to ring center). Very close to the ring they travel in almost opposite directions. Farther away they are nearly parallel. This may impact on dose calculations since these are sensitive to orientation. For off-site doses this effect should be small and results reported here are for parallel incidence of both 'beams'.

Fig. 7 shows maximum dose equivalent in a TEP embedded in soil in the orbit plane for relatively low energy col-

liders of 250 or 500 GeV per beam and for $2 \cdot 10^{20}$ decays per year as a function of distance from the center of the ring. The Fermilab dose limit is also indicated and it appears that there is no problem locating such a collider on the site of a typical accelerator laboratory. For 1 TeV and above this becomes more difficult as the situation in Fig. 8 depicts for $1.2 \cdot 10^{21}$ decays/year [21], although a 1 TeV (per ring) machine might still be accommodated if one uses the DOE criterion of 1 mSv/year. Note that in both Figs. 7 and 8 the muons are presumed to travel along a geometric circle thereby producing a uniform ν-dose everywhere around the ring.

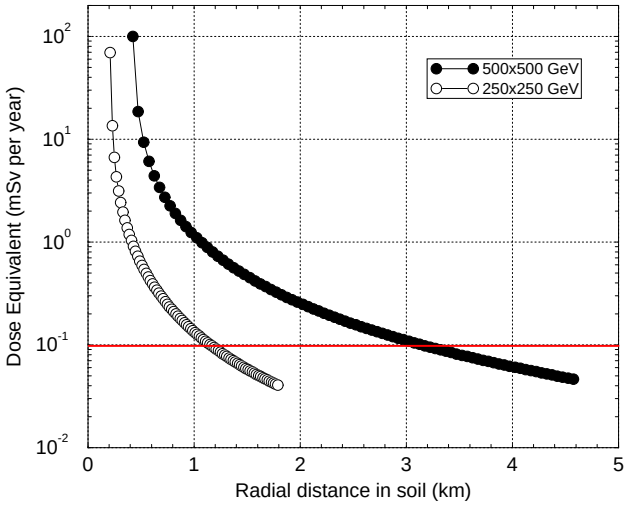

Figure 7: Maximum dose equivalent in TEP embedded in soil in low-energy muon collider orbit plane with 2×10^{20} decays per year *vs* distance from ring center.

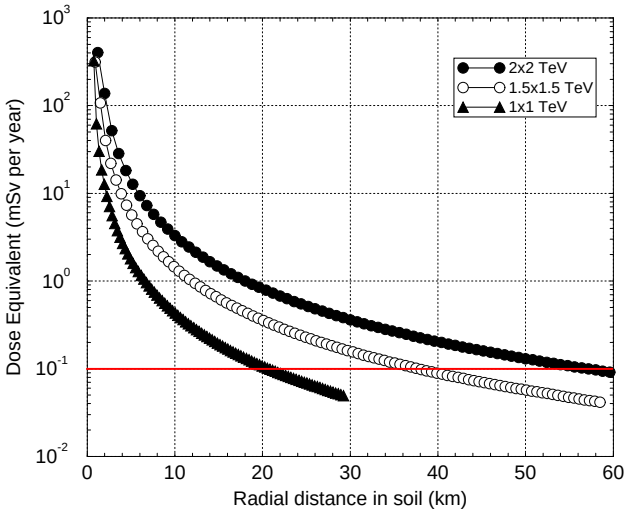

Figure 8: Maximum dose equivalent in TEP embedded in soil in high-energy muon collider orbit plane with 1.2×10^{21} decays per year *vs* distance from ring center.

Neutrino induced radiation from field-free regions (drifts, straight sections, etc.) becomes a most serious radiation problem at high energy muon colliders even over very short regions. Fig. 9 illustrates this for the dose calculated as a function of distance downstream of a 0.5 m long drift traversed by a 1.5 TeV muon beam and in which $2.6 \cdot 10^{16}$ muon decays occur per year. The off-site limit of 0.1 mSv/yr is met after 53 km. From geometrical considerations, dose grows linearly with drift length while it declines quadratically as a function of downstream distance. It increases with muon energy by the usual E^3 (see Introduction). For example, for a 10 TeV muon beam and only a 0.1 m drift with 10^{16} decays per year, the distance to reach the off-site limit is 380 km. Even a weak field applied to the drift mitigates the problem drastically which suggests that this be included in any serious design of a high energy muon collider.

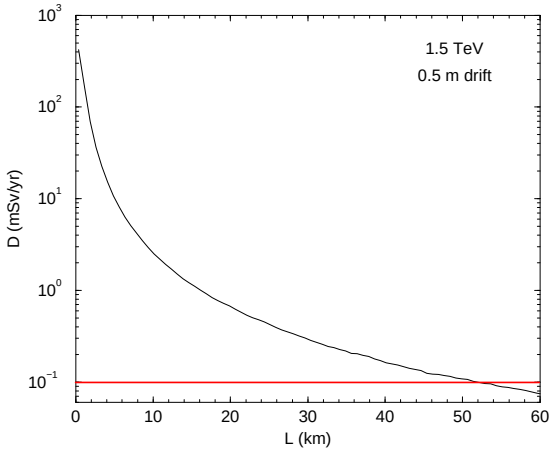

Figure 9: Maximum dose equivalent in TEP embedded in soil after a 0.5 m drift for a 1.5 TeV muon beam with $2.6 \cdot 10^{16}$ decays/year in that drift *vs* distance downstream.

The examples above show that the strictly circular model of a muon collider ring is seriously flawed. A better, but far more laborious, model should—in addition to the dipoles—include straight sections and drifts as well as quadrupoles, while the beam should be described by a realistic phase space distribution and undergo betatron oscillations. Vertical focusing/defocusing actions tend to dilute the dose similar to expressly induced 'wobbling' (see below) while in the horizontal plane it results in alternate dilution and concentration of the dose.

One proposed mitigation of the neutrino radiation problem is to place the collider deep underground. However, for practical purposes, the earth's curvature prevents this from being a generic solution to the problem. There is also the regulatory question whether delivering an off-site dose above the limit at *any* depth underground—or height above it—is permissible. With respect to this last point, the practice of purchasing easements from the affected property owners does not seem to present a workable solution —at least for existing labs and for TeV-scale collider—in

view of the large area to be covered. Regulatory matters aside, one can ask how deep underground a collider ring—with planar orbit—must be located to meet a certain limiting surface dose. Table 2 provides some answers for various muon collider rings (assuming suppressed contribution from the straight sections) at the annual decay rates indicated for both DOE and Fermilab limits. As can be seen the depths required to achieve the Fermilab standard are such that they may add considerably to overall cost and impose a substantial extra burden on conventional safety practices.

Table 2: *Depth, d, to reduce ν-induced long-term maximum dose at surface, (at radial distance, R, from center) to* DOE *and Fermilab annual off-site limits at N decays/yr.*

	$\sqrt{s}$ (TeV)	0.5	1	2	3	4
	$N\times10^{21}$	0.2	0.2	1.2	1.2	1.2
1 mSv	R (km)	0.4	1.1	6.5	12	18
	d (m)	$\leq$1	$\leq$1	3.3	11	25
0.1 mSv	R (km)	1.2	3.2	21	37	57
	d (m)	$\leq$1	$\leq$1	34	107	254

At any depth, mitigation may be achieved by beam wobbling, i.e., by expressly perturbing the orbit in the *vertical* plane to achieve the necessary dilution in dose delivered off-site. (As noted above, perturbation in the *horizontal* plane redistributes dose less evenly and thus counters mitigation. However, it may still be useful to help avoid a certain area, e.g., a nearby populated site or physics experiment.) To study wobbling a vertical wave is added to the muon orbit as an idealization of what might be done with an actual lattice [2, 22]. This wave or perturbation is expected to vary in strength and phase over the course of a year—perhaps aided by feedback from detectors in the field—so as to stay everywhere under the limit.

By way of illustration, Fig. 10 shows maximum dose for various levels of the vertical wave field. The curve labeled B=0.2 T, for example, corresponds to a 20 mrad roll in the ($\sim 8\ m$) arc dipoles which achieves a 200 μrad kick. It can be seen that dose delivered off site can be lowered by more than an order of magnitude or, alternatively, distance needed to achieve off-site limits may be reduced by as much as a factor of five. To avoid complications with skewed quadrupoles, net rolls are canceled before entering quadrupoles. Reverse dipole rolls and other changes can be executed from time to time to reduce average annual dose levels in all directions.

Other mitigation proposals mostly center around an 'alternative' site: an island or a mountain (of the right size and shape) which would permit the ν's to pass 'harmlessly above the surroundings' [3]. Analysis of such proposals best awaits nomination of a specific site. Quite possibly, one trades in the radiation problem for a different set of problems which, in the end, may be even less manageable. It is also not clear—as remarked upon in connection with underground doses—whether such proposals will withstand regulatory scrutiny.

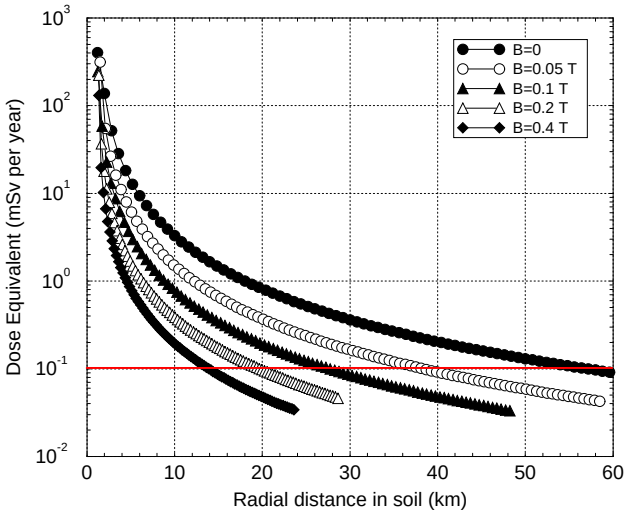

Figure 10: Maximum dose equivalent in TEP located in orbit plane *vs* distance from ring center in soil around a 2+2 TeV muon collider with 1.2×10^{21} decays per year for five values of vertical wave field.

7 CONCLUDING REMARKS

Minimizing off-site neutrino radiation is one of the main challenges to the design and civil engineering aspects of a high-energy muon collider or storage ring. The newly updated MARS provides a valuable tool to calculate the extent of the problem and study proposed mitigations. Results presented here show how dose depends strongly on muon energy and on the geometry between source and TEP. While pertaining to rather idealized situations, they should nonetheless be useful for assessing radiation problems associated with more specific designs and scenarios for muon colliders and storage rings. More detailed answers may be obtained by programming specific geometries and μ-beam characteristics into MARS. In particular, ν-radiation aspects of a collider in the TeV regime present a strong challenge with beam wobbling holding perhaps the most promise to significantly alleviate the problem. However, the realization of a high energy collider lies well into the future and this may also mean that improved techniques of beam cooling and steering allow the same or better luminosity to be reached with much lower currents—and much lower ν-radiation.

The regulatory question which arises so frequently as to whether one is free to deliver an over-the-limit dose deep underground or high up in the air eventually must be addressed within the legal framework of the community where the device is to be located. If the answer is negative, some regulatory relief—or interpretation of existing rules as applied to neutrinos—may well be necessary to proceed with a muon collider, given the realities of accelerator technology, budgets and siting options. Calculating whole-

body dose assuming a ν-fluence evenly distributed over the phantom, as discussed in Sec. III, is one example of how an interpretation specific to neutrino induced dose might be introduced. In discussing muon storage rings and colliders, results are presented in terms of maximum dose equivalent. As mentioned in Sec. IV, whole-body doses are about a factor of two lower with little dependence on neutrino energy, geometry, or composition of interposed material. Since meeting regulatory limits appears to be a challenge in some instances, such a seemingly modest factor might significantly reduce costs associated with radiation safety. Another example of regulatory relief might be to allow higher dose limits for ν-radiation in difficult-to-access off-site locations. But such relief or special interpretation can only be proposed seriously if it is defensible on strict grounds that it will harm no one. For this, the present program can be expected to provide a firm basis.

Future revisions of the MARS code may need to include neutrino oscillations and the like into the calculation—which likely entails a third set of cross sections for τ-neutrinos. At this date there is insufficient knowledge about oscillations to do so meaningfully. But, quite possibly, they may yet play a significant role in 'neutrino radiation safety'.

8 REFERENCES

[1] King, B. J., private communication (1996).

[2] Mokhov, N. V., Van Ginneken, A.: *"Muon Collider Neutrino Radiation"*, Muon Collider Collaboration Meeting Book, Orcas Island, WA (1997).

[3] King, B. J.: *Proc. 1999 Particle Accelerator Conf.*, p. 318 (1999).

[4] Mokhov, N. V., Van Ginneken, A.: *Proc. 1999 Particle Accelerator Conf.*, p. 3074 (1999).

[5] Cossairt, J. D., Grossman, N. L., Marshall, E. T.: *Fermilab-Conf-96/324* (1996) and *Fermilab-Pub-97/101* (1997).

[6] Mokhov, N. V.: *"The MARS Code System User's Guide, Version 13(95)"*, Fermilab-FN-628 (1995); *http://www-ap.fnal.gov/MARS/.*; Mokhov, N. V., et al.: Fermilab-Conf-98/379 (1998); LANL Report LA-UR-98-5716 (1998); *nucl-th/9812038 v2 16 Dec 1998*; *Proc. of the Fourt Workshop on Simulating Accelerator Radiation Environments (SARE4)*, Knoxville, TN, September 14-16, 1998, pp. 87-99.

[7] Particle Data Group: *Phys. Lett.*, **B204**, 1 (1988).

[8] Halzen, F., Martin, A. D.: *"Quarks and Leptons"*, Wiley, New York (1984).

[9] Perrier, F.: *"Precision Tests of the Standard Electroweak Model"*, P. Langacker, Ed., World Scientific, Singapore, 385 (1995).

[10] Llewellyn Smith, C. H.: *Phys. Rep.*, **3C**, 2499 (1981).

[11] Horstkotte, J., et al.: *Phys. Rev.*, **D25**, 2473 (1982).

[12] Tsai, Y.-S.: *Rev. Mod. Phys.*, **46**, 815 (1974).

[13] Panman, J.: *"Precision Tests of the Standard Electroweak Model"*, P. Langacker, Ed., World Scientific, Singapore, 504 (1995).

[14] Maiani, L.: *"Neutrino Physics"*, K. Winter, Ed., Cambridge, New York, 278 (1991).

[15] Drukier, A., Stodolsky, L.: *Phys. Rev.*, **D30**, 2473 (1984).

[16] Rein, D., Sehgal, L.: *Nucl. Phys.*, **B223**, 29 (1983); Marage , P., et al.: *Z. Phys.*, **C31**, 191 (1986) and *Z. Phys.*, **C43**, 523 (1989).

[17] To be precise: in calculations it is averaged over a phantom representing a human minus the arms and legs which are less radiation sensitive.

[18] Auxier, J. A., Snyder, W. S., Jones, T. D.: *"Radiation Dosimetry"*, Vol. I, Ch. 6, F.H. Attix and W.C. Roesch, Eds., Academic Press, New York (1968).

[19] Johnson, C., Rolandi, G., Silari, M.: *"Prospective Study of Muon Storage Rings at CERN"*, B. Autin, A. Blondel, and J. Ellis, Eds., *CERN 99-02, ECFA 099-197*, 105 (1999).

[20] Mokhov, N. V.: *Fermilab-Conf-96/367*, (1996).

[21] It is assumed total number of muons per store, hence total decays per year, increases with energy to counter the decline in cross section with energy ($\propto s^{-1}$).

[22] Johnstone, C. J., Mokhov, N. V.: *Proc. 1997 Particle Accelerator Conf.*, p. 414 (1997).